

Supporting Information

**Low-Temperature Access to Active Iron and Iron/Nickel Nitrides as Potential
Electrocatalysts for the Oxygen Evolution Reaction**

*Christopher R. DeLaney, Sergio Diaz-Abad, Shamus O’Leary, Anna Gonzàlez-Rosell, Ulises
Martinez[#], Sandip Maurya, Sergei A. Ivanov, John Watt**

C. R. DeLaney, S. L. O’Leary, S. A. Ivanov, J. Watt

Center for Integrated Nanotechnologies

Materials Physics and Applications Division

Los Alamos National Laboratory

Los Alamos, New Mexico 87545, USA

S. Diaz Abad, U. Martinez[#], S. Maurya,

Materials Synthesis and Integrated Devices,

Materials Physics and Applications Division.

Los Alamos National Laboratory,

Los Alamos, New Mexico 87545, United States

[#]Current Address: Sandia National Laboratories, Albuquerque, New Mexico 87185, United States

Email: watt@lanl.gov

Keywords: transition metal nitride, oxygen evolution reaction (OER), electrocatalysis, cluster, nanoparticles.

Experimental Methods

1.1. Chemicals.

Iron pentacarbonyl ($\text{Fe}(\text{CO})_5$) was purchased from Strem Chemicals. Tetraethylammonium chloride ($(\text{NEt}_4)\text{Cl}$) was obtained from Alfa Aesar. Oleylamine (OLA, 98% purity) was purchased from 2A Biotech and used without further purification. Acetone and diethylenetriamine (DETA) were purchased from Acros Organics. Dimethylformamide (DMF), dichloromethane (DCM), chloroform, ethanol (EtOH), methanol (MeOH), isopropanol (IPA), NaOH, MgSO_4 , and AgNO_2 were purchased from Sigma-Aldrich. Triiron dodecacarbonyl ($\text{Fe}_3(\text{CO})_{12}$), acetonitrile (MeCN), tetrahydrofuran (THF), hexanes, toluene, diethyl ether (Et_2O), and urea were purchased from Thermo Fisher Scientific. NEt_4NO_2 was prepared as previously described.¹ The multigram quantities of $(\text{NMe}_4)_2[\text{Ni}_6(\text{CO})_{12}]$ were generously provided by late Prof. Larry Dahl (UW-Madison), who synthesized the cluster according to a previously reported procedure.^{2, 3} All syntheses involving metal carbonyl precursors were conducted under an inert N_2 atmosphere using either a Schlenk line or a glovebox.

1.2. Synthetic procedures

Optimized synthesis of $\text{Fe}_3\text{N}_{1.08}$. $\epsilon\text{-Fe}_3\text{N}_{1.08}$ NPs were prepared by dissolving 200 mg (0.40 mmol) of $\text{Fe}_3(\text{CO})_{12}$ in 5 mL of DMF pre-saturated with urea (666 mg, 11 mmol) via extended sonication (40 mins). This solution was then added dropwise at 2 mL h^{-1} using a syringe pump into a reaction flask containing 24 mL of degassed OLA held at 270°C , stirred at 500 rpm under nitrogen using mechanical stirrer. After the addition, the mixture was held at 270°C for 1 hour, cooled to 80°C , and precipitated by adding a 1:1 mixture of degassed toluene and methanol via cannula. Particles were magnetically separated, and the supernatant was removed via cannula. The particles were washed by suspending in toluene and magnetically separated three times. The flask was evacuated and transferred into a glovebox for storage.

Synthesis of $\text{Fe}_3\text{N}_{0.93}$ NPs. $\epsilon\text{-Fe}_3\text{N}_{0.93}$ NPs were synthesized by dissolving 153 mg (0.22 mmol) of $(\text{NEt}_4)[\text{Fe}_4\text{N}(\text{CO})_{12}]$ in 3 mL of DMF pre-saturated with urea (333 mg, 5.54 mmol). The solution was injected at 4 mL/h via syringe pump into 8 mL of degassed OLA at 270°C and stirred at 500 rpm under nitrogen. The reaction proceeded for 1 hour post-addition, was cooled to 80°C , and NPs

were precipitated as above. Washing and storage procedures were identical to those used for $\text{Fe}_3\text{N}_{1.08}$.

Optimized synthesis of $\text{Fe}_{1.94}\text{Ni}_{1.06}\text{N}$. $\text{Fe}_{1.94}\text{Ni}_{1.06}\text{N}$ NPs were prepared by dissolving 61 mg (0.07 mmol) of $(\text{NMe}_4)_2[\text{Ni}_6(\text{CO})_{12}]$ and 100 mg (0.13 mmol) of $(\text{NEt}_4)[\text{Fe}_4\text{N}(\text{CO})_{12}]$ in 10 mL of MeCN as previously described by Pergola *et al.*⁴, stirred for 72 hours. The dark brown solution was then taken to dryness, and the resulting solid was dissolved in 4.5 mL of DETA. It was injected at 5 mL/h into 12 mL of degassed OLA 290°C. The remainder of the procedure was identical to that of $\text{Fe}_3\text{N}_{1.08}$.

Synthesis of Nitride-Containing Precursors

Synthesis of $(\text{NEt}_4)[\text{Fe}(\text{CO})_3(\text{NO})]$. The cluster was synthesized following a procedure adapted from Gladfelter *et al.*⁵ First, 1.5 mL (11.1 mmol) of $\text{Fe}(\text{CO})_5$ was added dropwise to a chilled suspension of $(\text{NEt}_4)\text{NO}_2$ (1506 mg, 8.5 mmol) in 60 mL of degassed THF. After addition, an oil bubbler was fitted to the flask to allow for CO/CO_2 loss and the mixture was stirred overnight at room temperature. The volume was then reduced to ~10 mL *in vacuo*, filtered through Celite, and precipitated with Et_2O . The resulting yellow/orange solid was washed repeatedly with Et_2O until the supernatant was clear. The product was then dried *in vacuo* and stored in a glovebox $(\text{NEt}_4)[\text{Fe}(\text{CO})_3(\text{NO})]$. Yield: 87% (2117 mg, 7.4 mmol). FT-IR (THF): $\nu(\text{CO}) = 1978 \text{ s}, 1875 \text{ vs}, 1643 \text{ s cm}^{-1}$.

Synthesis of $(\text{NEt}_4)[\text{Fe}_4\text{N}(\text{CO})_{12}]$. The cluster was synthesized following a procedure adapted from Fjare *et al.*⁶ $(\text{NEt}_4)[\text{Fe}(\text{CO})_3(\text{NO})]$ (520 mg, 1.7 mmol) and $\text{Fe}_3(\text{CO})_{12}$ (1496 mg, 3.0 mmol) were loaded in a 125 mL Schlenk flask in a glovebox.⁶ The solids dissolved in 50 mL of degassed THF and stirred overnight at room temperature. The solution had changed color from dark green to brown. The resulting solution was dried *in vacuo*, dissolved in MeOH, filtered, and dried again. The dark brown solid was loaded into a glovebox for storage. Yield: 79% (963 mg, 1.4 mmol). FT-IR (THF): $\nu(\text{CO}) = 2016 \text{ s}, 1991 \text{ vs}, 1964 \text{ m}, 1933 \text{ w cm}^{-1}$.

Synthesis of $\text{HFe}_4\text{N}(\text{CO})_{12}$. Following the procedure adapted from Tachikawa *et al.*⁷, $\text{Na}[\text{Fe}_4\text{N}(\text{CO})_{12}]$ (800 mg, 1.34 mmol) was suspended in hexanes and treated with ~5 mL of 85%

H₃PO₄ aqueous solution. After 20 minutes, the complex dissolved forming a protonated analogue in the organic layer. The layers were separated, and brown-colored organic layer was filtered through celite and dried over anhydrous MgSO₄ overnight. The dried solution was filtered and evaporated to yield dark brown/black solid of HFe₄N(CO)₁₂. Yield: 24.6% (191 mg, 0.33 mmol). FT-IR (n-hexanes): $\nu(\text{CO}) = 2053 \text{ vs}, 2035 \text{ s}, 2023 \text{ s}, 2016 \text{ w(sh)}, 1999 \text{ w(sh)}, 1992 \text{ m}, 1968 \text{ w}.$

1.3. Characterization

The FT-IR spectra were collected on a Thermo Nicolet Nexus 670 FT-IR with either an ATR probe (solids) or ZnSe flow cell (solutions). XRD (θ -2 θ scans) was performed using a Rigaku SmartLab II diffractometer (Cu K α) in parallel beam geometry. TEM was collected using a Titan Environmental TEM and a Tecnai F30 TEM, both operated at 300 keV. Magnetic measurements were obtained with a Quantum Systems vibrating sample magnetometer (VSM). The ICP data were acquired using an Agilent Technologies ICP-OES 5110.

Electrochemical testing was performed in a half-cell using 0.1M NaOH or 1M KOH as supporting electrolytes under constant nitrogen bubbling. The working electrode was a 5 mm diameter glassy carbon disk; a hydrogen reference electrode was used. Potentials were referenced to RHE using the following equation:

$$E(\text{RHE}) = E(\text{Hg}/\text{HgO}) + 0.098 + 0.059 * pH \quad \text{eq.1}$$

LSV scans were run from 0.7V to 1.75V vs RHE at 5 mVs⁻¹, overpotential was evaluated at 10 mA cm⁻² for 1h; stability tests were conducted at 1.85 V vs RHE during 24 h. Tafel slopes were extracted from LSVs using equation:

$$\mu = a * \log\left(\frac{i}{i_0}\right) \quad \text{eq.2}$$

Where μ is the overpotential or overpotential, a is the Tafel slope, i the current density, and i_0 the exchange current density.

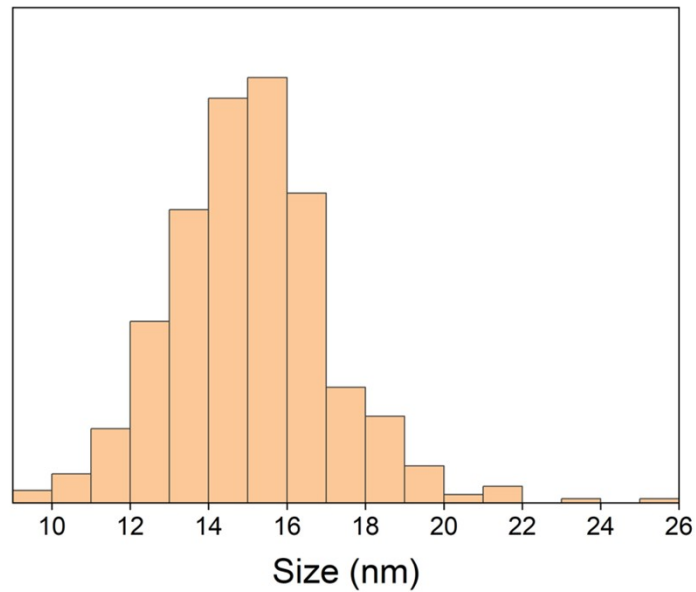


Figure S1. Histogram of particle sizing data for Fig. 1b. The NPs are measured to be 15.0 nm in size with a polydispersity of 2.1%.

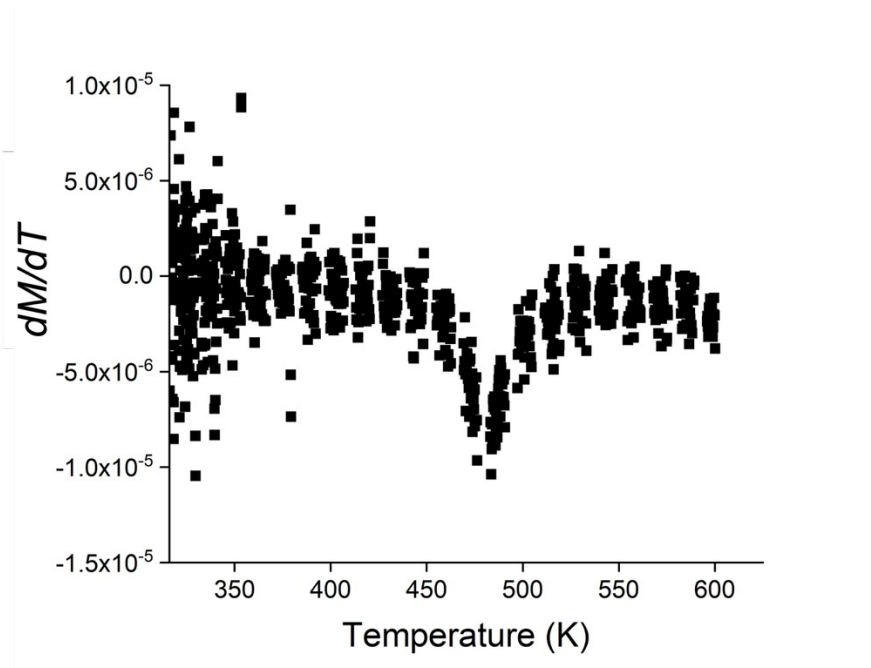


Figure S2. Plot of dM/dT as a function of T for the as synthesized ϵ -Fe₃N_{1.08} NPs, indicating a T_C of 480 K.

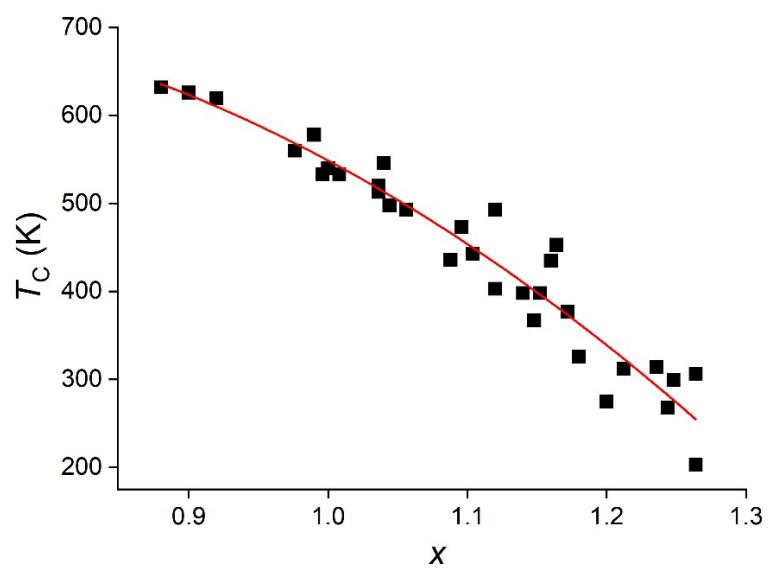


Figure S3. Literature values for the Curie temperature (T_C) of various compositions of ϵ - Fe_3N_x as a function of x .^{8,9}

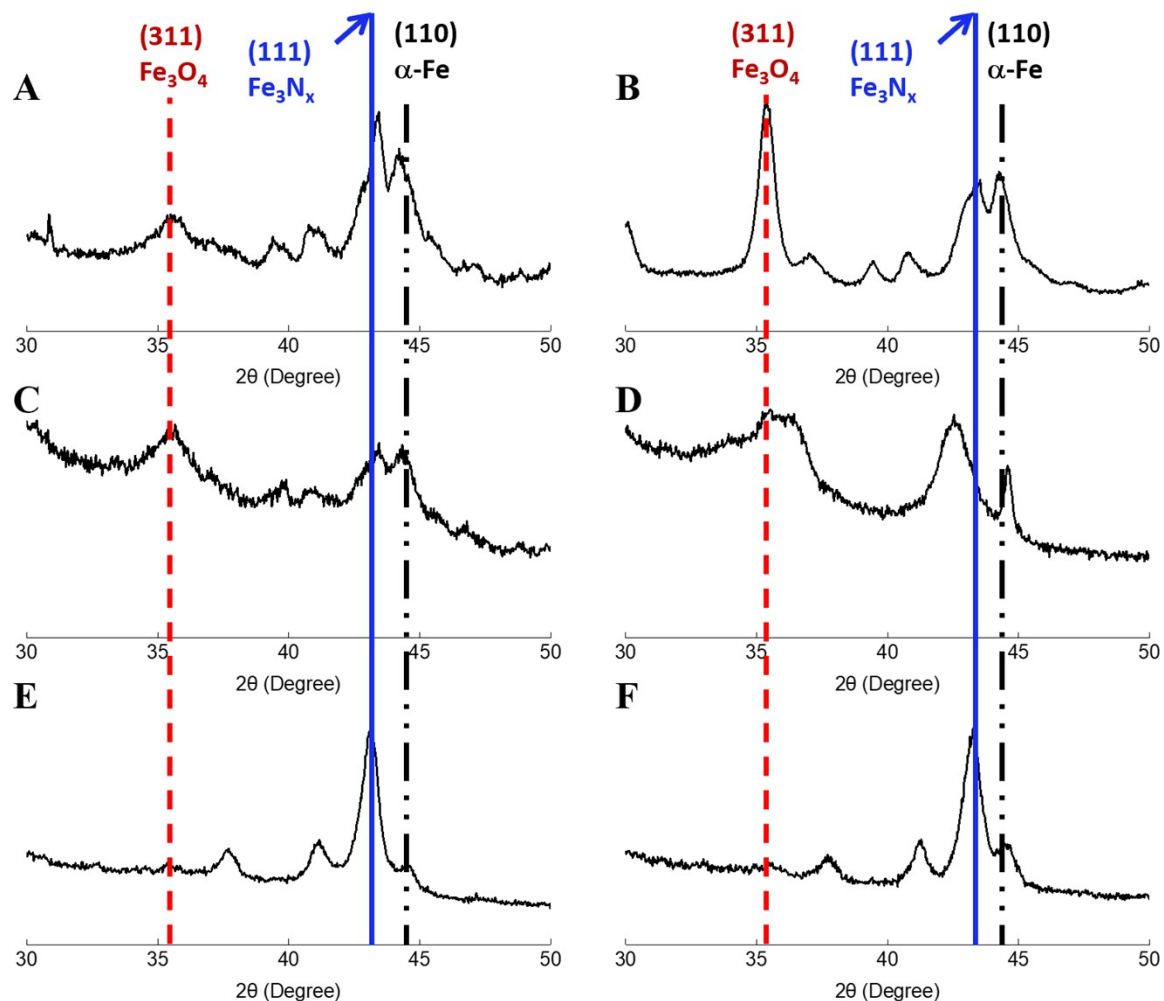


Figure S4. XRD pattern of products from the thermal decomposition of $\text{Fe}_3(\text{CO})_{12}$ at 270 °C in following hot solvent/cluster solvent mixtures; (A) oleylamine (OLA)/dimethylformamide (DMF), (B) octadecene (ODE)/DMF, (C) OLA/OLA, (D) ODE/OLA, (E) OLA/diethylenetriamine (DETA), and (F) ODE/DETA. In each case, the reaction was carried out without an additional source of nitrogen. The reference position of the (111) reflection of $\epsilon\text{-Fe}_3\text{N}_x$ is shown in blue solid line. The (110) reflection of $\alpha\text{-Fe}$ is in black dot-dash, and the (311) of iron oxide is in red dash. For the experiments with DETA, 100 mg of $\text{Fe}_3(\text{CO})_{12}$ were dissolved in 3 mL of DETA and injected into 8 mL of OLA or ODE at 270 °C.

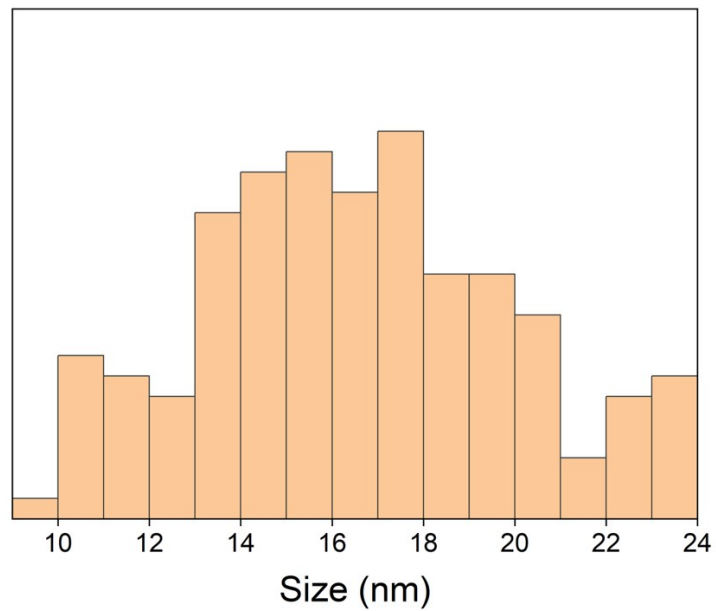


Figure S5. Histogram of particle sizing data for Fig. 3b. The particles are measured to be 16.6 nm in size with a polydispersity of 4.9%.

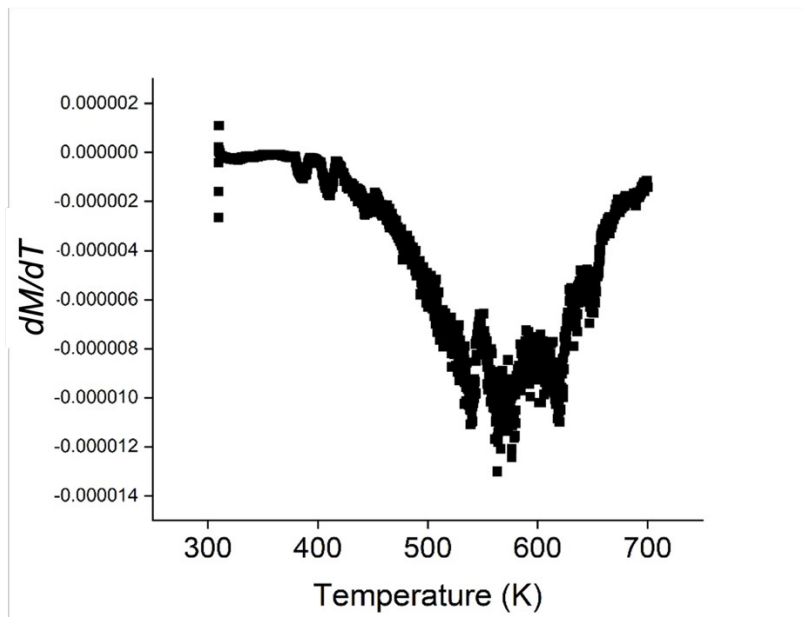


Figure S6. Plot of dM/dT as a function of T for the as synthesized ϵ -Fe₃N_{0.93} NPs, indicating a T_C of 598 K.

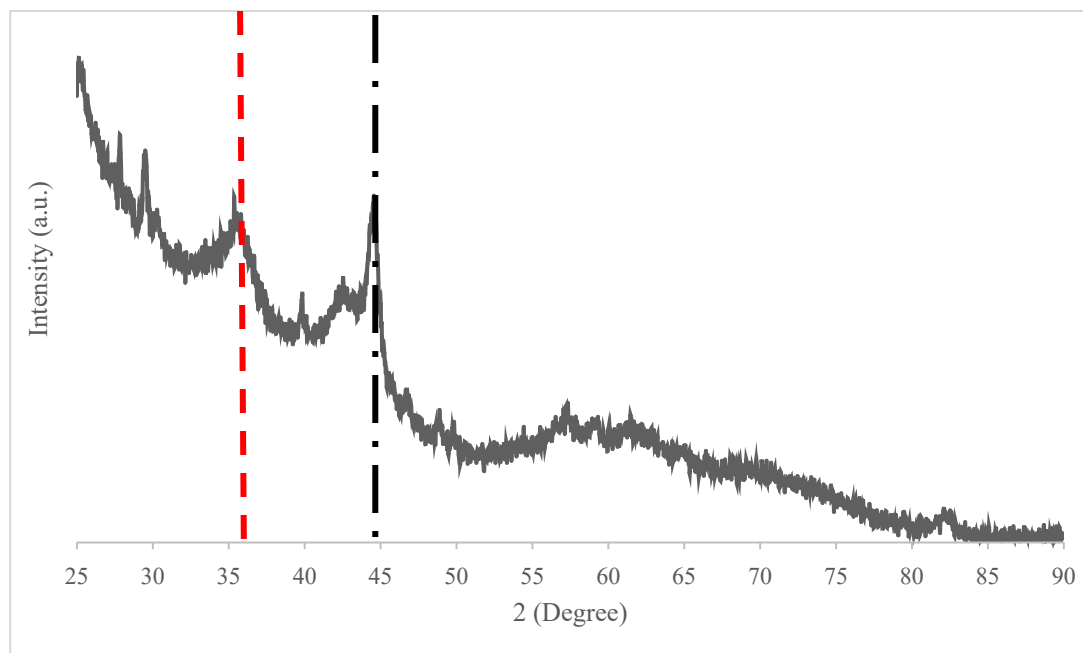


Figure S7. XRD pattern of a product obtained after dropwise addition of $\text{HFe}_4\text{N}(\text{CO})_{12}$ in DMF/urea. This solution was added to OLA at 200°C over 1 hour followed by an additional hour of incubation. The reference position of the (311) reflection of iron oxide is shown in the red dashed line, while (110) reflection of $\alpha\text{-Fe}$ is in black dot-dash.

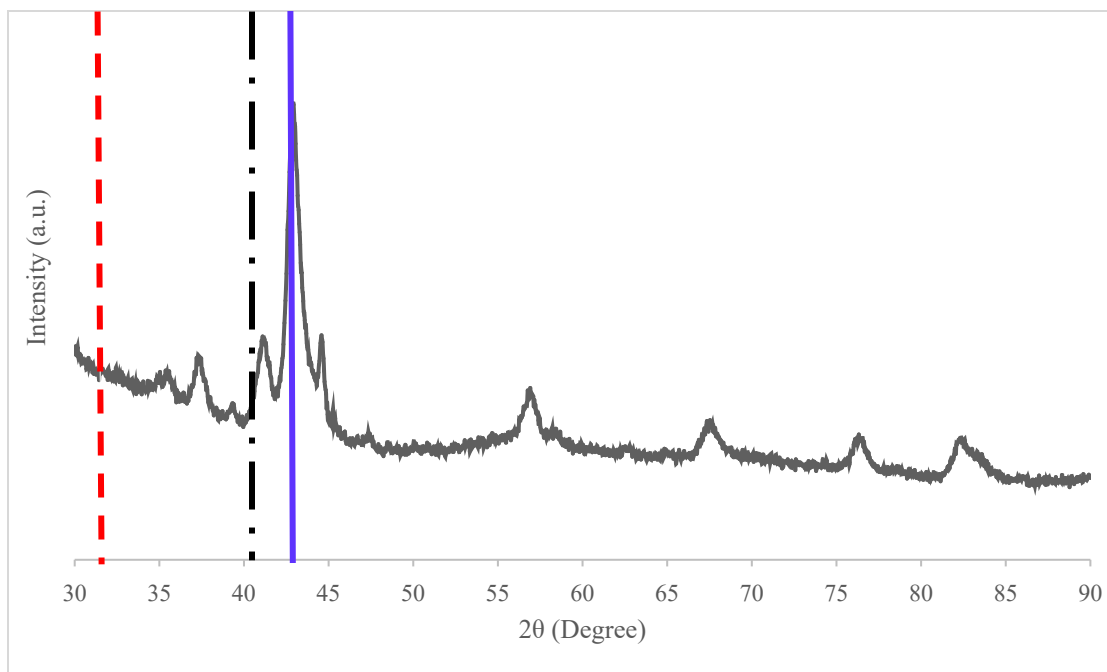


Figure S8. XRD pattern of particles obtained after dropwise addition of $\text{HFe}_4\text{N}(\text{CO})_{12}$ in DMF with 28-fold excess of urea. This solution was added into OLA at 270 °C over 1 hour followed by an additional hour of incubation. The reference position of the (111) reflection of $\epsilon\text{-Fe}_3\text{N}_x$ is shown in blue solid line. The (110) reflection of $\alpha\text{-Fe}$ is in black dot-dash and the (311) of iron oxide is in red dash.

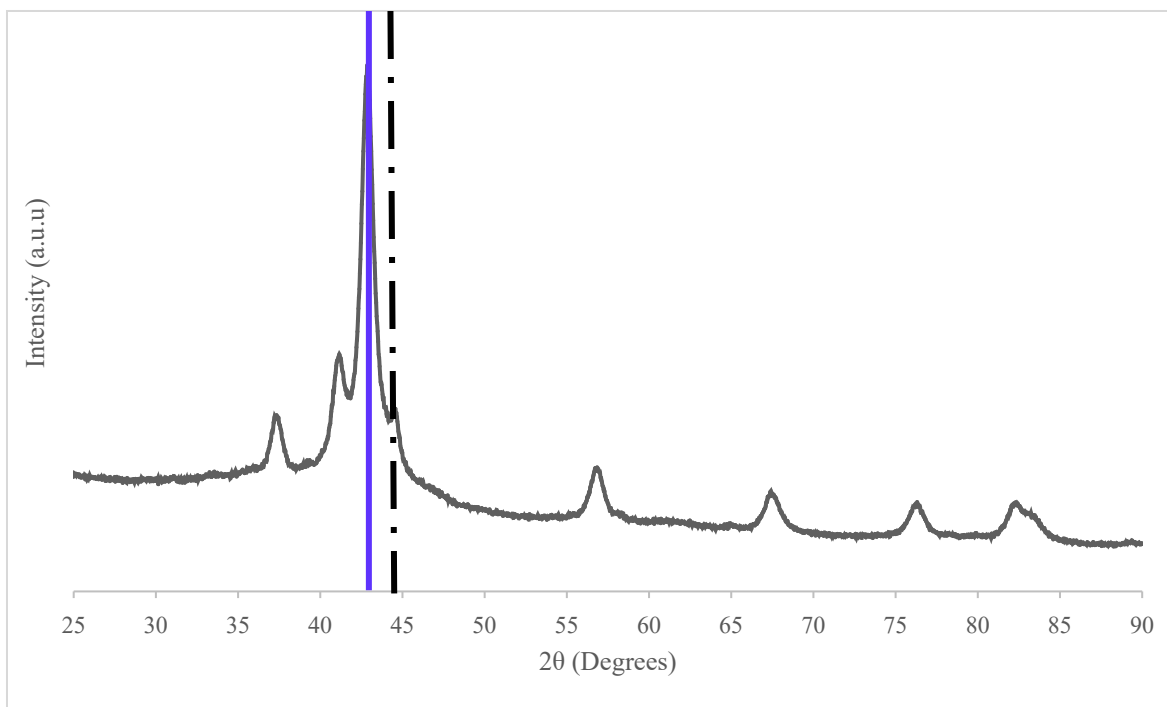


Figure S9. XRD pattern of particles synthesized via dropwise addition of $(\text{NEt}_4)[\text{Fe}_4\text{N}(\text{CO})_{12}]$ dissolved in DETA. The solution was added to OLA at 270 °C over 1 hour followed by an hour of incubation. The reference position of the (111) reflection of $\epsilon\text{-Fe}_3\text{N}_x$ is shown in blue solid line. The (110) reflection of $\alpha\text{-Fe}$ is in black dot-dash.

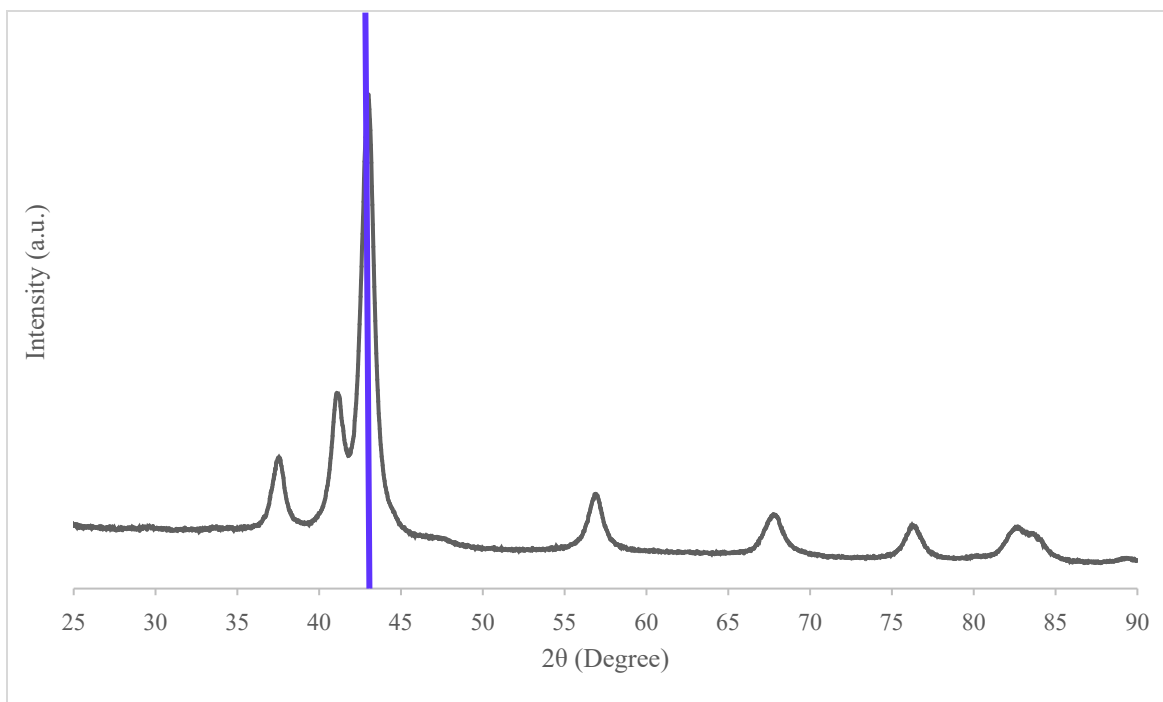


Figure S10. XRD pattern of particles obtained after dropwise addition of $\text{HFe}_4\text{N}(\text{CO})_{12}$ dissolved in DETA. This solution was added to OLA at 270 °C over 1 hour followed by an hour of incubation. The pattern fit best to $\epsilon\text{-Fe}_3\text{N}$ with the reference peak of the (111) shown as blue solid line.

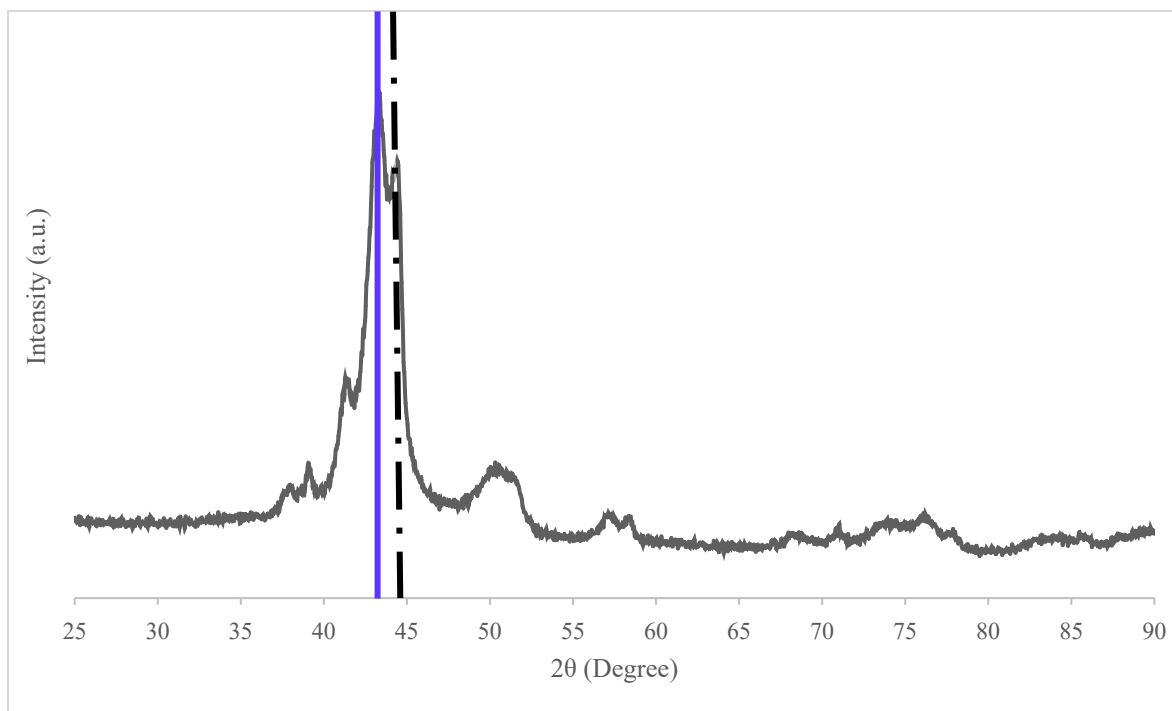


Figure S11. XRD pattern of mix-metal product obtained after dropwise addition of a mixture of $(\text{NMe}_4)_2[\text{Ni}_6(\text{CO})_{12}]$ and $[\text{NEt}_4][\text{Fe}_4\text{N}(\text{CO})_{12}]$ at a 1:2 ratio in DMF with a 28-fold excess of urea. This solution was added to OLA at 290°C over 1 hour followed by an hour of incubation. The reference position of the (111) reflection of $\text{Fe}_{0.73}\text{Ni}_{0.27}\text{N}_{0.33}$ is shown as a blue solid line. The (110) reflection of NiFe (taenite) is in black dot-dash.

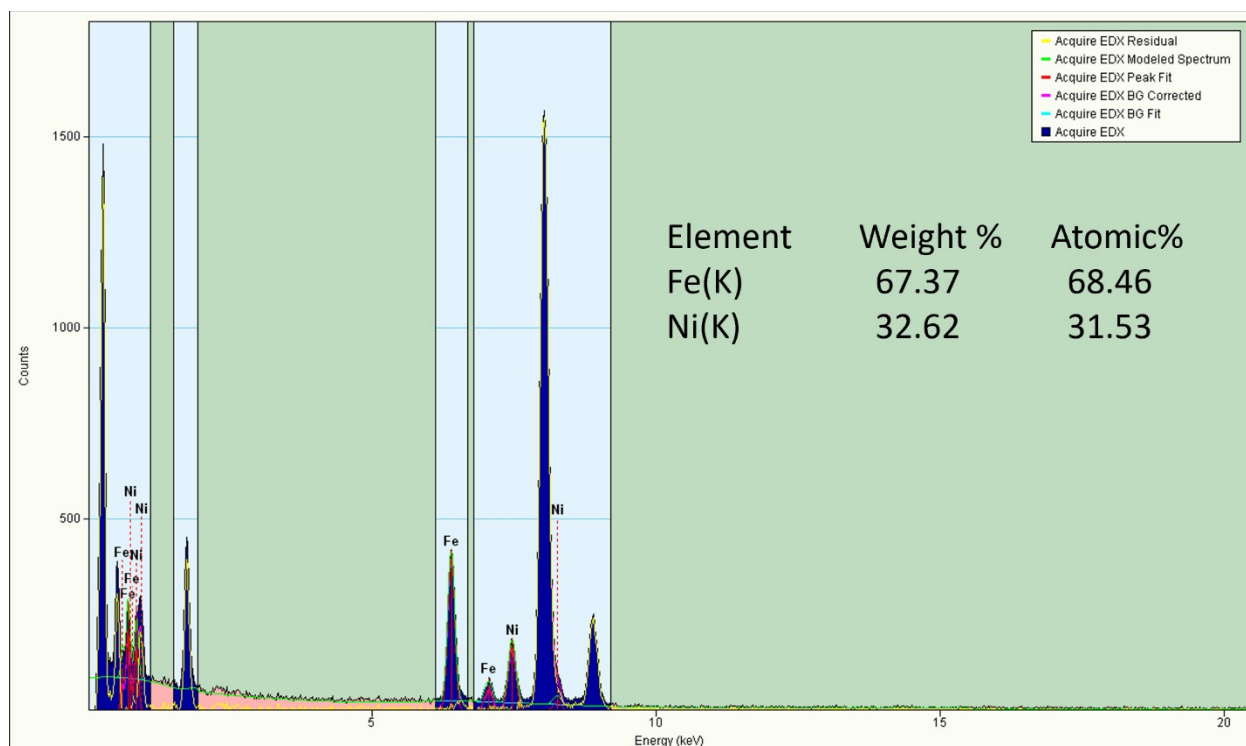


Figure S12. X-ray energy dispersive spectra (XEDS) of $\text{Fe}_{1.94}\text{Ni}_{1.06}\text{N}$ NPs.

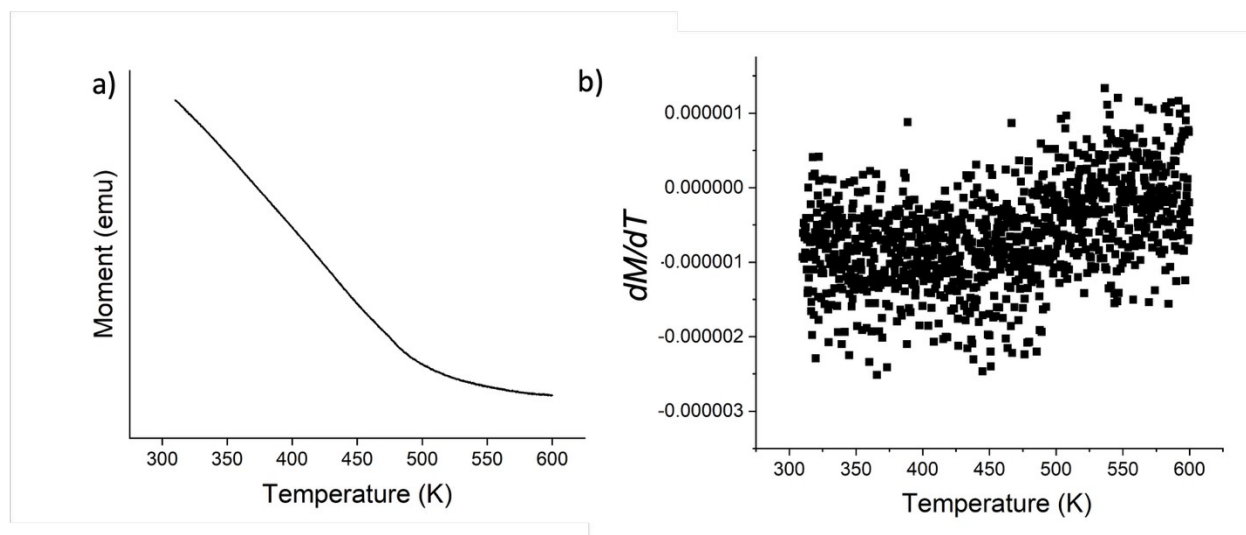


Figure S13. (a) M vs T plot and the corresponding (b) dM/dT vs T plot of NPs (see main text). A lack of a distinct onset, and relatively shallow slope curve in (a) are a result of the broad size distribution and small size of the nanoparticles, which introduce a larger contribution from surface effects. However, the derivative in (b) indicates a T_C of around 450 K.

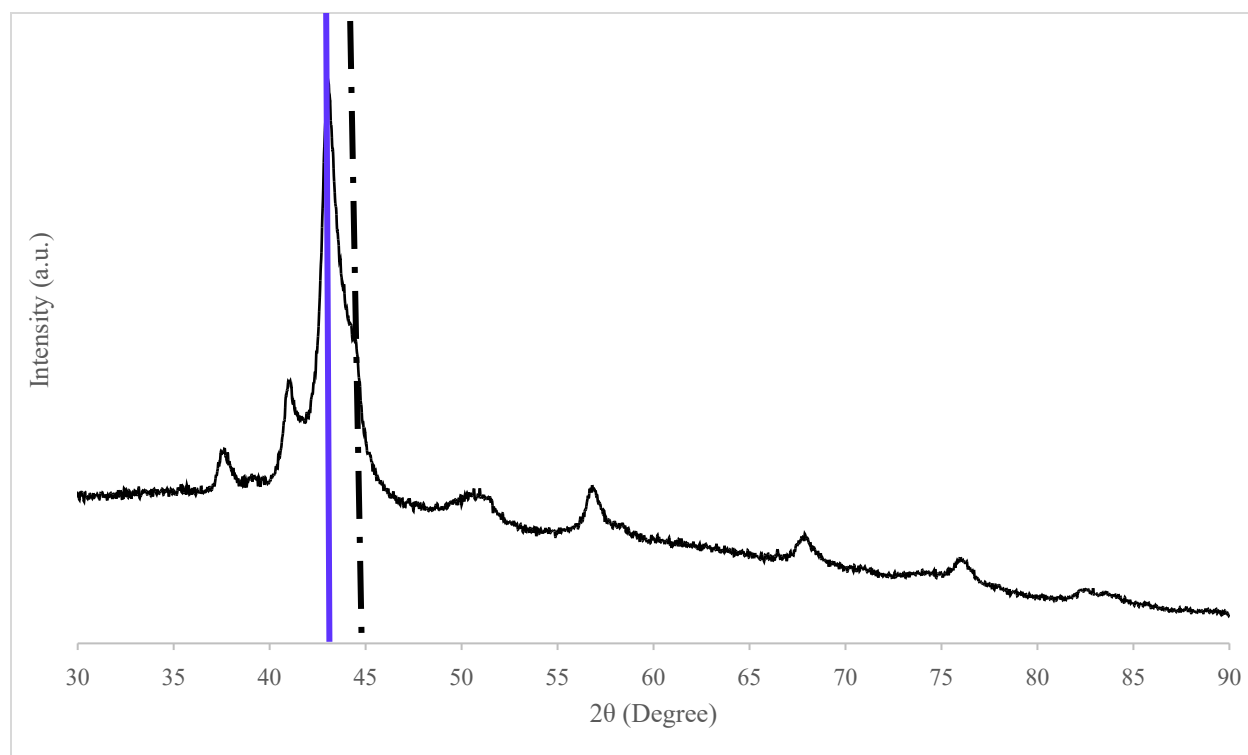


Figure S14. XRD pattern of particles synthesized via dropwise addition of a mixture of $(\text{NMe}_4)_2[\text{Ni}_6(\text{CO})_{12}]$ and $\text{Fe}_3(\text{CO})_{12}$ (1:2 ratio) in DMF with a 28-fold excess of urea. The solution was added to OLA at 290°C over 1 hour followed by an hour of incubation. The reference position of the (111) reflection of $\text{Fe}_{0.73}\text{Ni}_{0.27}\text{N}_{0.33}$ is shown as a blue solid line. The (110) reflection of NiFe (taenite) is in black dot-dash.

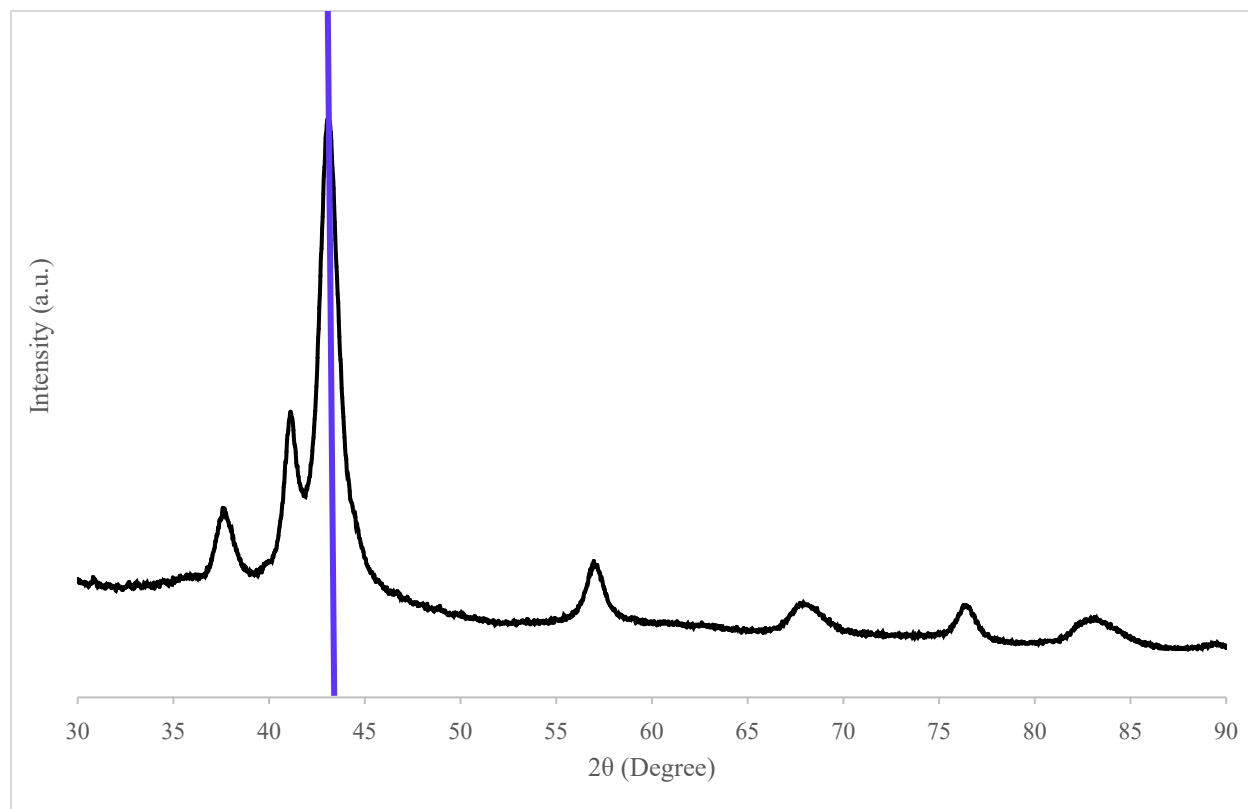
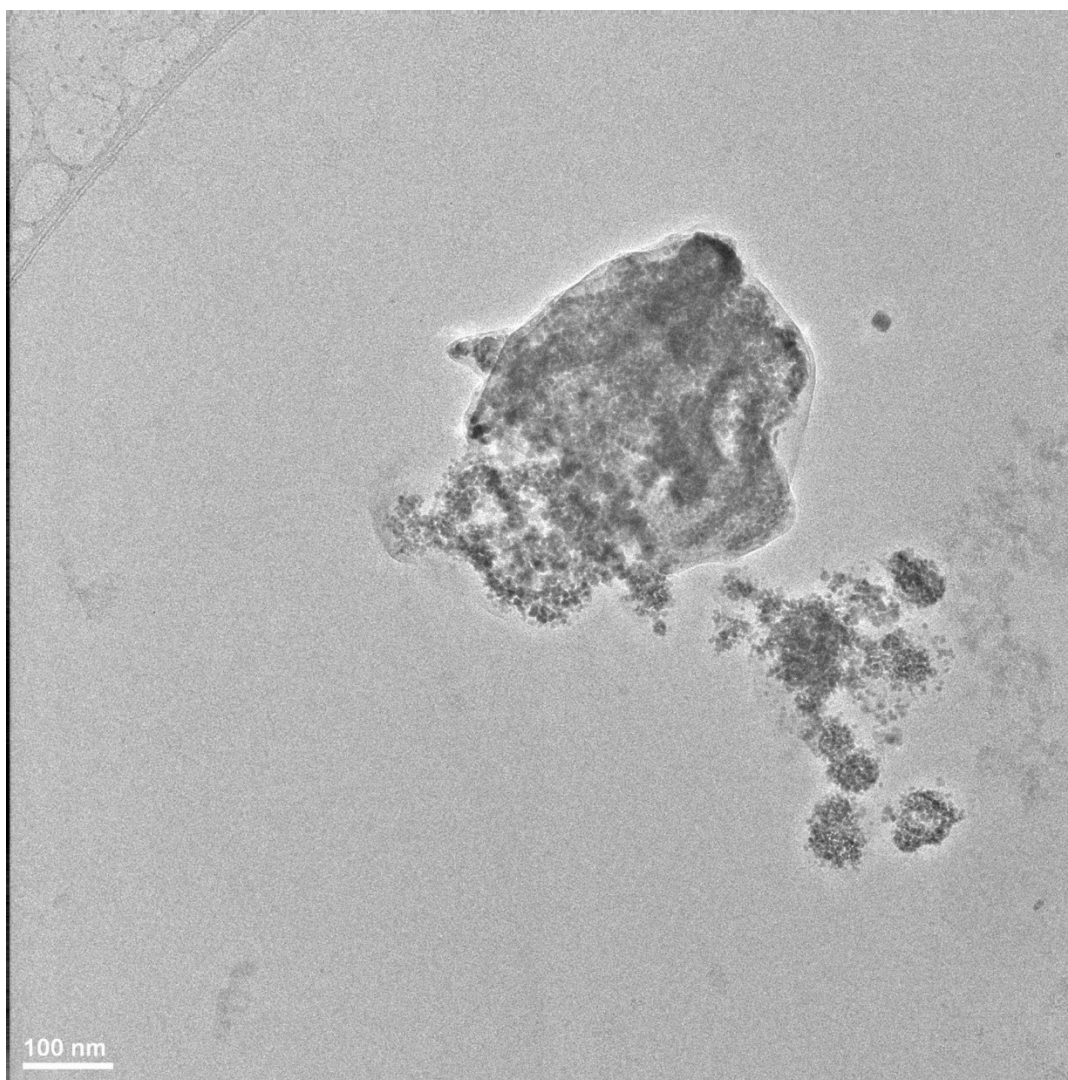


Figure S15. XRD powder pattern of NPs synthesized via dropwise addition of a solution containing $(\text{NMe}_4)_2[\text{Ni}_6(\text{CO})_{12}]$ and $\text{Fe}_3(\text{CO})_{12}$ at a 1:2 ratio in DETA. This solution was added 290°C OLA over the course of 1 hour followed by an additional hour of incubation. The reference position of the (111) reflection of $\text{Fe}_{0.73}\text{Ni}_{0.27}\text{N}_{0.33}$ is shown as a blue solid line.



Electrode	
$\text{Fe}_3\text{N}_{1.08}$	5
$\text{Fe}_3\text{N}_{0.93}$	3
$\text{Fe}_{1.94}\text{Ni}_{1.06}\text{N}$	4
RuO_2	8

Tabl

Figure S16. TEM image of NPs resulting from the one-pot synthesis (see main text). In short, particles were synthesized via dropwise addition of a mixture of $(\text{NMe}_4)_2[\text{Ni}_6(\text{CO})_{12}]$ and $\text{Fe}_3(\text{CO})_{12}$ (1:2 ratio) in DETA. This solution was added to OLA at 290°C over 1 hour followed by an hour of incubation.

Figure S17. Tafel slope data for $\text{Fe}_3\text{N}_{1.08}$, $\text{Fe}_3\text{N}_{0.93}$ and $\text{Fe}_{1.94}\text{Ni}_{1.06}\text{N}$ NPs along with industry standard RuO_2 and IrO_2 . Electrode: 5 mm glassy carbon (GC) disk electrode spinning at 800 rpm; Electrolyte: 1M KOH.

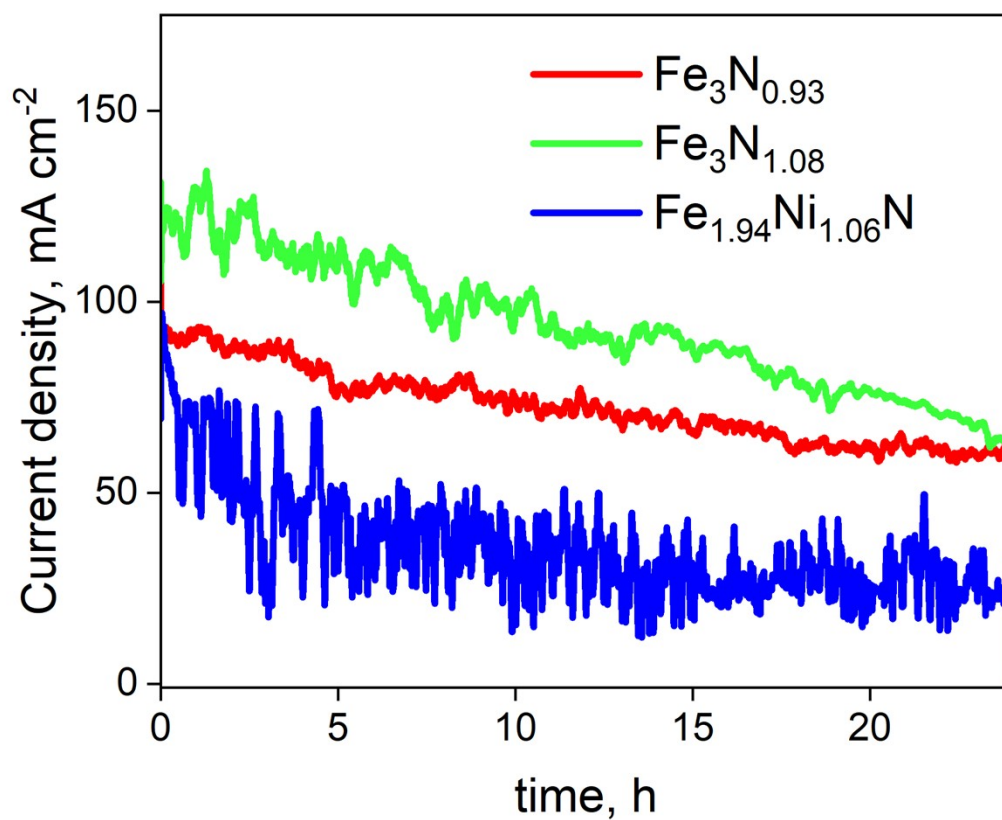


Figure S17. 24h preliminary durability testing of current density vs time for the ϵ -Fe₃N_{0.93}, ϵ -Fe₃N_{1.08}, and Fe_{1.94}Ni_{1.06}N NPs at 1.8V vs RHE.

References:

1. K. Tanaka, R. Wakita and T. Tanaka, *J. Am. Chem. Soc.*, 2002, **111**, 2428-2433.
2. J. C. Calabrese, L. F. Dahl, A. Cavalieri, P. Chini, G. Longoni and S. Martinengo, *J. Am. Chem. Soc.*, 1974, **96**, 2616-2618.
3. G. Longoni, P. Chini and A. Cavalieri, *Inorganic Chemistry*, 1976, **15**, 3025-3029.
4. R. Della Pergola, M. Bruschi, F. Fabrizi de Biani, A. Fumagalli, L. Garlaschelli, F. Laschi, M. Manassero, M. Sansoni and P. Zanello, *C. R. Chim.*, 2005, **8**, 1850-1855.
5. R. E. Stevens and W. L. Gladfelter, *Inorganic Chemistry*, 2002, **22**, 2034-2042.
6. D. E. Fjare and W. L. Gladfelter, *Inorganic Chemistry*, 2002, **20**, 3533-3539.
7. M. Tachikawa, J. Stein, E. L. Muettert, R. G. Teller, M. A. Beno, E. Gebert and J. M. Williams, *J. Am. Chem. Soc.*, 2002, **102**, 6648-6649.
8. H. A. Wriedt, N. A. Gokcen and R. H. Nafziger, *Bulletin of Alloy Phase Diagrams*, 1987, **8**, 355-377.
9. Y. Li, D. Pan, Y. Zhou, Q. Kuang, C. Wang, B. Li, B. Zhang, J. Park, D. Li, C. Choi and Z. Zhang, *Nanoscale*, 2020, **12**, 10834-10841.